Mode of Action of the Antibacterial Cecropin B2: A Spectrofluorometric Study†

Ehud Gazit,‡ Won-Jae Lee,§ Paul T. Brey,§ and Yechiel Shai*,‡

Department of Membrane Research and Biophysics, The Weizmann Institute of Science, Rehovot, 76100 Israel, and Unité d'Ecologie des Systems Vectoriels, Institut Pasteur, 25 rue du Dr. Roux, 75724 Paris Cedex 15, France

Received March 16, 1994; Revised Manuscript Received July 7, 1994®

ABSTRACT: Cecropin B2 (CecB) is a 35 amino acid residue, antibacterial peptide that was isolated from the hemolymph and cuticular matrix of the silkworm, *Bombyx mori.* Synthetic peptides with sequences corresponding to CecB and its truncated analogue, [3→35]CecB, were synthesized and selectively labeled at their N-terminal amino acids with either 7-nitrobenz-2-oxa-1,3-diazol-4-yl (NBD) or rhodamine fluorescent probes. Utilization of these probes facilitated study of the interaction of cecropin with model phospholipid membranes at a high lipid/peptide molar ratio (~3000:1), permitting investigation of the initial steps involved in this process. The surface partition coefficient of CecB, derived from binding isotherms of the NBD-labeled peptide, was 10-fold higher with acidic phospholipids than with zwitterionic ones, which correlates with the high efficiency of CecB and its analogues in permeating acidic phospholipid vesicles. Furthermore, a direct correlation was found between the antibacterial activity of CecB or its truncated analogues and the ability of their Rho-labeled analogues to interact with bacteria and human red blood cells. We propose that CecB binds phospholipid membranes preferentially as monomers lying on the surface, rather than cooperatively as bundles that form transmembranal pores via a "barrel stave" mechanism. This is based on the following: (i) the linearity of CecB's binding isotherms; (ii) the low energy transfer between membrane-embedded donor and acceptor-labeled CecB, even in the presence of a transmembrane potential; (iii) the surface localization of CecB's N-terminus; (iv) the need for more than 100 peptide molecules per phospholipid vesicle to induce initial ion leakage; and (v) the fact that CecB is a highly positively charged amphipathic α-helix, and therefore it is not expected to transverse the membrane as a monomer. We speculate that the non-cooperative binding of the peptides on the outer surface of the bacteria (i.e., no aggregation of CecB monomers) may help them to diffuse efficiently into the inner membrane, which is thought to be the target of antibacterial peptides.

Cecropins are highly potent, inducible antibacterial peptides that were originally isolated from the immune hemolymph of the moth *Hyalophora cecropia* (Hultmark et al., 1980; Steiner et al., 1981) and that play an important role in insect immunity (Boman, 1991; Hultmark, 1993). Cecropins have also been isolated from the immune hemolymph of other Lepidopteran and Dipterian insects [for a review, see: Boman and Hultmark, 1987; Hultmark, 1993], from the small intestines of pigs (Lee et al., 1989), and recently from the cuticular matrix of the abraded integument of the silkworm *Bombyx mori* (Brey et al., 1993; Lee & Brey, 1994). These findings imply that cecropins are widespread in the animal kingdom and are synthesized by various tissues. The primary structure of the major cuticular cecropin is identical to that of cecropin B2 of the hemolymph of *B. mori* (Morishima et al., 1990; Lee & Brey, 1994). The insect cecropins are peptides of 35–39 amino acids that have a highly positively charged N-terminal region and a hydrophobic C-terminus. The structure of one type of cecropin, cecropin A of *Hyalophora cecropia*, as determined by two-dimensional NMR[1] spectroscopy in a hydrophobic environment, consists of a helix–bend–helix motif [an amphipathic α-helical N-terminus, a glycine–proline bend, and a hydrophobic C-terminal α-helix (Holak et al., 1988)]. The amphipathic α-helical structure of the N-terminus of this cecropin is important for its antibacterial activity, since the introduction of a helix-breaking amino acid, proline, into this region considerably reduces this activity (Andreu et al., 1985). Moreover, deletion of the first two amino acids of cecropin A or replacement of the highly conserved tryptophan in position 2 with a charged amino acid causes a 10–80-fold or more decrease in its antibacterial activity (Andreu et al., 1985). The C-termini of the insect cecropins end with an α-amide group, which is also important for their antibacterial activity, whereas the C-terminus of the pig cecropin is not amidated.

The antibacterial spectrum of cecropins is broad and includes both Gram-negative and Gram-positive bacteria. Cecropins do not lyse erythrocytes, a characteristic of other antibacterial amphipathic α-helical peptides such as magainin (Zasloff, 1987) and dermaseptin (Mor et al., 1991), which were isolated from frog skin. Although the mode of action of cecropin and other antibacterial peptides is not yet fully understood, their antibacterial activity appears to be due to their permeation of membranes via peptide–lipid interaction, rather than to receptor-mediated recognition. This is supported by the finding that analogues of cecropin and magainin that contain

† This research was supported in part by the Israel Cancer Association, the Basic Research Foundation administered by the Israel Academy of Sciences and Humanities, the Pasteur Institute, and the Korean POSCO Scholarship Society. Y.S. is the incumbent of the Adolpho and Evelyn Blum Career Development Chair in Cancer Research.

* Author to whom correspondence should be addressed: telephone 972-8-342711; Fax 972-8-344112.

‡ The Weizmann Institute of Science.

§ Institut Pasteur.

® Abstract published in *Advance ACS Abstracts,* August 15, 1994.

[1] Abbreviations: Boc, butyloxycarbonyl; CecB, cecropin B2; DCC, dicyclohexylcarbodiimide; DIEA, *N,N*-diisopropylethylamine; diS-C_2-5, 3,3′-diethylthiodicarbocyanine iodide; DMSO, dimethyl sulfoxide; HEPES, *N*-(2-hydroxyethyl)piperazine-*N*′-2-ethanesulfonic acid; HOBT, 1-hydroxybenzotriazole; HF, hydrogen fluoride; LPS, lipopolysaccharides; NBD, 7-nitrobenz-2-oxa-1,3-diazol-4-yl; NBD-F, 4-fluoro-7-nitrobenz-2-oxa-1,3-diazole; Rho, tetramethylrhodamine; NMR, nuclear magnetic resonance; Pam, (phenylacetamido)methyl; PC, egg phosphatidylcholine; PS, phosphatidylserine; RP-HPLC, reverse phase high-performance liquid chromatography; SUV, small unilamellar vesicles; TFA, trifluoroacetic acid; TFE, trifluoroethanol.

0006-2960/94/0433-10681$04.50/0

only D-amino acids possess antibacterial activity indistinguishable from that of the parent molecules (Wade et al., 1990; Bessalle et al., 1990). Phospholipid model membranes are widely used to investigate the membrane-permeating properties of antibacterial peptides. The membrane-permeating capacity of cecropins has been explained by either channel formation or membrane destabilization (Christensen et al., 1988; Okada & Natori, 1985; Steiner et al., 1988; Durell et al., 1992), utilizing single-channel experiments or leakage of vesicle content studies.

In this article, the synthesis, fluorescent labeling, and interaction with phospholipid membranes and bacteria of cecropin B2 (CecB) derived from *B. mori* and its truncated [3→35] analogue are described. Labeling of the peptides with 7-nitrobenz-2-oxa-1,3-diazol-4-yl (NBD) or rhodamine facilitated examination of the initial steps of the interaction of CecB with phospholipid membranes at high lipid/peptide molar ratios (>3000:1), ratios at which as few as 2–4 CecB molecules are bound to a single, small unilamellar vesicle. The NBD probe facilitated the determination of the locations of the N-termini of the peptides in their membrane-bound states, the nature of the binding (simple adhesion or cooperative), and the calculation of their surface partition coefficients. Fluorescence energy transfer experiments, performed with NBD (an energy donor) or rhodamine (an energy acceptor) labeled CecB, facilitated the study of CecB's organization in a membrane-bound state. Rho labeling of the peptides also facilitated their visualization upon binding to bacteria and human erythrocytes.

Our results reveal a non-cooperativity in the binding of CecB to phospholipid membranes and an inability to associate on the surface of acidically charged membranes independent of membrane polarization. This suggests that CecB binds phospholipid membranes preferentially as monomers lying on the surface, rather than as bundles that form a transmembrane pore. The advantage of this non-cooperative binding mode of interaction in preventing the aggregation of cecropins on the surface of outer bacterial membranes, and therefore in assisting them in efficiently diffusing into the inner target membranes, is discussed in line with proposed mechanisms for the antibacterial activity of other amphipathic antibacterial peptides.

EXPERIMENTAL PROCEDURES

Materials. *p*-Methylbenzhydrylamine resin was purchased from Applied Biosystems (Foster City, CA), and butyloxycarbonyl (Boc) amino acids were obtained from Peninsula Laboratories (Belmont, CA). Other reagents used for peptide synthesis included trifluoroacetic acid (TFA, Sigma), *N,N*-diisopropylethylamine (DIEA, Aldrich, distilled over ninhydrin), dicyclohexylcarbodiimide (DCC, Fluka), 1-hydroxybenzotriazole (HOBT, Pierce), and dimethylformamide (peptide synthesis grade, Biolab). Egg phosphatidylcholine (PC) and phosphatidylserine (PS) from bovine spinal cord (sodium salt, grade I) were purchased from Lipid Products (South Nutfield, U.K.). Cholesterol (extra pure) was supplied by Merck (Darmstadt, Germany) and recrystallized twice from ethanol. 3,3′-Diethylthiodicarbocyanine iodide (diS-C_2-5) and 5(and 6)-carboxytetramethylrhodamine succinimidyl ester were obtained from Molecular Probes (Eugene, OR). 4-Fluoro-7-nitrobenz-2-oxa-1,3-diazole (NBD-F) was obtained from Sigma. All other reagents were of analytical grade. Buffers were prepared in double-glass-distilled water.

Peptide Synthesis and Purification. The CecB and [3→35]-CecB peptides were synthesized by a solid phase method on *p*-methylbenzhydrylamine resin (0.05 mequiv; Merrifield et al., 1982). The resin-bound peptides were cleaved from the resins by hydrogen fluoride (HF) and finally extracted with dry ether after HF evaporation. These crude peptide preparations contained one major peak, as revealed by RP-HPLC, that was >80% pure peptide by weight. The synthesized peptides were further purified by RP-HPLC on a C_4 reverse phase Vydac semipreparative column (300-Å pore size). The column was eluted in 40 min, using a linear gradient of 15–80% acetonitrile in water containing 0.1% TFA (v/v) and a flow rate of 1.8 mL/min. The purified peptides were shown to be homogeneous (~99%) by analytical HPLC. The peptides were subjected to amino acid analysis and automatic animo acid sequencing using a gas phase automatic sequencer (Applied Biosystems Model 477A) equipped with an on-line PTH amino acid analyzer (Model 120A).

Fluorescent Labeling of Peptides. Labeling of the N-terminus of the CecB and [3→35]CecB peptides with fluorescent probes was achieved by labeling the resin-bound peptides as previously described (Rapaport & Shai, 1991). Briefly, 10 mg of resin-bound peptides (3–4 μmol) were treated with TFA (50% (v/v) in methylene chloride), in order to remove the Boc protecting group from the N-terminal amino groups of the linked peptides. The resin-bound peptides were then reacted with either (i) carboxytetramethylrhodamine succinimidyl ester (3–4 equiv) in dry dimethylformamide containing 2.5% (v/v) diisopropylethylamine or (ii) NBD-F in dry dimethylformamide. The peptides were then cleaved from the resins by HF and finally precipitated with ether. All peptides were purified using RP-HPLC as described in the previous section.

Antibacterial Activity of Cecropin B and Its Analogues. The antibacterial activity of synthetic CecB, [3→35]CecB and the fluorescently labeled CecB derivatives was assessed by an inhibition zone assay using thin agarose plates seeded with bacteria (Hultmark et al., 1982): *Escherichia coli* MC 4100, *Bacillus megaterium* 51.17, *Micrococcus luteus* 53.45 (=U.S. FDA strain PCI 1001), *Serratia marcescens* 15.88 isolated from *Anopheles gambiae*, and *Pseudomonas aeruginosa* A22. All of these bacteria were obtained from the Pasteur Institute Collection. Serial dilutions of known amounts of the synthetic CecB, [3→35]CecB, Rho-CecB, NBD-CecB, and Rho-[3→35]CecB were made for each bacterium. Antibacterial activities were expressed as the lowest lethal concentration of cecropin or its derivatives that inhibits growth of the respective bacterium in thin agarose plates.

Binding of the Peptides to Bacteria and Erythrocytes. *In vitro* binding experiments were conducted on the highly cecropin sensitive *E. coli*, the cecropin resistant insect pathogen *Serratia marcescens*, and the cecropin insensitive human erythrocyte of blood group AB^+. Early stationary phase *E. coli* and *S. marcescens*, ca. 10^6 cells, were incubated separately with Rho/ethanolamide (12.5 μM), Rho-CecB (12.5 μM), and Rho-[3→35]CecB (12.5 μM), respectively, in 20 μL of PBS (pH 7.5) for 10 min at room temperature and subsequently centrifuged at 15000*g* for 2 min. The bacteria were then washed twice in 5 μL of PBS (pH 7.5). Human erythrocytes (10^6 cells) were treated in an identical fashion with Rho/ethanolamide (12.5 μM), Rho-CecB (12.5 μM), or Rho-[3→35]CecB (12.5 μM), except that they were centrifuged at only 2500*g* for 5 min. The resulting bacteria and erythrocyte preparations were observed using a PolyVar 2 Reichert-Jung microscope with Nomarski differential interference phase contrast and fluorescence optics. Kodak Ektachrome 400 was used for all photomicrographs, and an

exposure time of 22 s was used for all fluorescent photomicrographs.

Detection of Proteolytic Activity in the Supernatant of S. marcescens' Culture Medium. S. marcescens was cultured in heart brain broth at 37 °C for 24 h. The culture was then centrifuged at 10000*g* for 10 min. Five aliquots of the resulting culture supernatant were each mixed with 2 μg of the synthetic CecB peptide (final volume of 25 μL). Each aliquot was incubated for a defined time period, after which the mixture was heat treated at 100 °C for 5 min and centrifuged at 15000*g* for 1 min. A control experiment was carried out using sterile heart brain broth instead of culture supernatant. Fifteen microliters of each sample was applied to the *E. coli* antibacterial assay plate as described above. The relative activity was expressed as a ratio of the inhibition zones in millimeters obtained by CecB dissolved in the cultured medium vs the sterile medium.

Preparation of Liposomes. Small unilamellar vesicles (SUV) were prepared by sonication of PC or PC/PS (1:1, w/w). Briefly, dry lipid and cholesterol (10:1, w/w) were dissolved in a $CHCl_3$/MeOH mixture (2:1, v/v). The solvents were then evaporated under a stream of nitrogen, and the lipids (at a concentration of 7.2 mg/mL) were subjected to a vacuum for 1 h and then resuspended in the appropriate buffer by vortexing. The resultant lipid dispersions were then sonicated for 5–15 min in a bath type sonicator (G1125SP1 sonicator, Laboratory Supplies Company Inc., New York) until clear. The lipid concentrations of the resulting preparations were determined by phosphorus analysis (Bartlett, 1959). Vesicles were visualized using a JEOL JEM 100B electron microscope (Japan Electron Optics Laboratory Co., Tokyo, Japan) as follows. A drop of vesicles was deposited on a carbon-coated grid and negatively stained with uranyl acetate. Examination of the grids demonstrated that the vesicles were unilamellar with an average diameter of 20–50 nm (Papahadjopoulos & Miller, 1967).

CD Spectroscopy. The CD spectra of the peptides were measured with a Jasco J-500A spectropolarimeter after calibrating the instrument with (+)-10-camphorsulfonic acid. The spectra were scanned at 23 °C in a capped, quartz optical cell with a 0.5 mm path length. Spectra were obtained at wavelengths of 250 to 190–200 nm. Seven scans were taken at a scan rate of 20 nm/min for each peptide. The peptides were scanned at concentrations of 2.0×10^{-5} M in methanol and in buffer (50 mM Na_2SO_4/25 mM HEPES–sulfate, pH 6.8) in the presence of phospholipid SUV. Fractional helicities (Greenfield & Fasman, 1969; Wu et al., 1981) were calculated as follows:

$$f_h = \frac{([\theta]_{222} - [\theta]^0_{222})}{[\theta]^{100}_{222}}$$

where $[\theta_{222}]$ is the experimentally observed mean residue ellipticity at 222 nm, and the values for $[\theta^0_{222}]$ and $[\theta^{100}_{222}]$, which correspond to 0% and 100% helix content at 222 nm, are estimated at 2000 and 30 000 deg·cm^2/dmol, respectively (Chen et al., 1974; Wu et al., 1981).

NBD Fluorescence Measurements. NBD-labeled peptide (0.2 nmol) was added to 2 mL of buffer (50 mM Na_2SO_4/25 mM HEPES–sulfate, pH 6.8) containing 800 nmol of PC or PS/PC SUV to establish a lipid/peptide ratio (4000:1) in which all of the peptide is bound to lipids. After a 2 min incubation, the emission spectrum of the NBD group was recorded (in three separate experiments) using a Perkin-Elmer LS-50B spectrofluorometer, with excitation set at 470 nm (10 nm slit).

Binding of Peptides to Vesicles. Binding experiments were conducted as previously described (Rapaport & Shai, 1991). Briefly, PC or PC/PS SUV was added successively to 0.2 μM fluoroscently labeled peptide at 25 °C. Fluorescence intensity was measured as a function of the lipid/peptide molar ratio on a Perkin-Elmer LS-50B spectrofluorometer, with excitation set at 470 nm, using a 10 nm slit, and emission set at 530 nm, using a 5 nm slit, in three separate experiments. To correct for the background signal contributed by the lipids to any given signal, the readings observed when unlabeled peptide was titrated with lipid vesicles were subtracted from each recording of fluorescence intensity.

The binding isotherms were analyzed as a partition equilibrium (Beschiaschvili & Seelig, 1990; Rapaport & Shai, 1991; Rizzo et al., 1987; Schwarz et al., 1986, 1987), using the following formula:

$$X_b = K_p C_f$$

where X_b is defined as the molar ratio of bound peptide (C_b) per total lipid (C_L), K_p corresponds to the partition coefficient, and C_f represents the equilibrium concentration of free peptide in the solution. In practice, it was assumed that the peptides initially were partitioned only over the outer leaflet (60%) of the SUV (Beschiaschvili & Seelig, 1990). Therefore, the partition equation becomes

$$X_b^* = K_p^* C_f$$

where X_b^* is defined as the molar ratio of bound peptide per 60% of total lipid and K_p^* is the estimated surface partition constant. The curve resulting from plotting X_b^* vs free peptide, C_f, is referred to as the conventional binding isotherm.

Resonance Energy Transfer (RET) Measurements. Fluorescence spectra were obtained at room temperature in a Perkin-Elmer LS-50B spectrofluorometer, with the excitation monochromator set at 460 nm to minimize the excitation of tetramethylrhodamine, with a 5-nm slit width. Measurements were performed in a 1 cm path length glass cuvette and a final reaction volume of 2 mL. In a typical experiment, donor (NBD-labeled) peptide at a final concentration of 0.1 μM was added to a dispersion of PC or PS/PC SUV (100 μM) in buffer (50 mM Na_2SO_4/25 mM HEPES–sulfate, pH 6.8), followed by the addition of acceptor (Rho-labeled) peptide in several sequential doses. Fluorescence spectra were obtained before and after the addition of the acceptor peptide. Changes in the fluorescence intensity of the donor due to processes other than energy transfer to the acceptor were determined by substituting unlabeled peptide for the acceptor and by measuring the emission spectrum of the acceptor alone in the presence of vesicles.

The efficiency of energy transfer (E) was determined by measuring the decrease in the quantum yield of the donor as a result of the addition of acceptor. E was determined experimentally from the ratio of the fluorescence intensities of the donor in the presence (I_{da}) and in the absence (I_d) of the acceptor at the donor's emission wavelength, after correcting for membrane light scattering and the contribution of acceptor emission. The percentage of transfer efficiency (E) is defined as

$$E = (1 - I_{da}/I_d)100$$

The correction for light scattering was made by subtracting the signal obtained when unlabeled analogues were added to

Table 1: Amino Acid Sequences of the Peptides and Their Fluorescently Labeled Analogues

peptide no.	designation	sequence
1	CecB	H_2N-R W K I F K K I E K M G R N I R D G I V K A G P A I E V L G S A K A I-NH_2
2	NBD-CecB	**NBD**-HN-R W K I F K K I E K M G R N I R D G I V K A G P A I E V L G S A K A I-NH_2
3	Rho-CecB	**Rho**-HN-R W K I F K K I E K M G R N I R D G I V K A G P A I E V L G S A K A I-NH_2
4	[3→35]CecB	H_2N-K I F K K I E K M G R N I R D G I V K A G P A I E V L G S A K A I-NH_2
5	NBD-[3→35]CecB	**NBD**-HN-K I F K K I E K M G R N I R D G I V K A G P A I E V L G S A K A I-NH_2
6	Rho-[3→35]CecB	**Rho**-HN-K I F K K E E K M G R N I R D G I V K A G P A I E V L G S A K A I-NH_2

vesicles containing the donor molecule. Correction for the contribution of acceptor emission was made by subtracting the signal produced by the acceptor-labeled analogue alone.

Membrane Permeation Induced by the Peptides. Membrane permeation was assessed by utilizing the diffusion potential assay (Loew et al., 1983; Sims et al., 1974) as previously described (Shai et al., 1990, 1991). In a typical experiment, in a glass tube, 4 μL (28.8 μg) of a liposome suspension, prepared in a K^+-containing buffer (50 mM K_2SO_4/25 mM HEPES–sulfate, pH 6.8), was diluted in 1 mL of an isotonic K^+-free buffer (50 mM Na_2SO_4/25 mM HEPES–sulfate, pH 6.8), to which the fluorescent, potential sensitive dye, diS-C_2-5, was then added. Valinomycin (1 μL of 10^{-7} M) was added to the suspension in order to slowly create a negative diffusion potential inside the vesicles, which led to a quenching of the dye's fluorescence. Once the fluorescence had stabilized, 3–10 min later, peptides were added. The subsequent dissipation of the diffusion potential, as reflected by an increase in fluorescence, was monitored on a Perkin-Elmer LS-50B spectrofluorometer, with excitation set at 620 nm and emission at 670 nm and the gain adjusted to 100%. The percentage of fluorescence recovery, F_t, was defined as

$$F_t = (I_t - I_0/I_f - I_0)100$$

where I_0 is the initial fluorescence, I_f is the total fluorescence observed before the addition of valinomycin, and I_t is the fluorescence observed after adding the peptide at time t.

RESULTS

To gain insight into the mode of action of the antibacterial CecB isolated from the silkworm *B. mori*, we investigated the initial steps involved in its interaction with phospholipid membranes. CecB, its truncated form [3→35]CecB, and their fluorescent derivatives were synthesized and characterized both spectroscopically and functionally. Fluorescently labeled analogues, selectively labeled at their N-terminal amino acid residues, were prepared by modifying the peptides with NBD (to serve as an energy donor and to facilitate binding experiments) or tetramethylrhodamine (to serve as an energy acceptor). The peptides and their designations are listed in Table 1.

CD Spectroscopy. The extent of α-helical secondary structures in CecB and [3→35]CecB was estimated from their CD spectra in a hydrophobic environment (methanol) and in buffer containing phospholipid PC/PS SUV (Figure 1). Both CecB and [3→35]CecB exhibited a mean residual ellipticity $[\theta]_{222}$ of −25 440 deg·cm²/dmol in methanol, which corresponds to a high fractional helicity value of 74% (Wu et al., 1981). This implies that the deletion of the two N-terminal amino acids of CecB has no effect on its secondary structure in an aprotic solvent. These values of fractional helicities are similar to those obtained with synthetic CecA and its analogues (Andreu et al., 1985). Similarly, high α-helical contents are present in other naturally occurring membrane-permeating

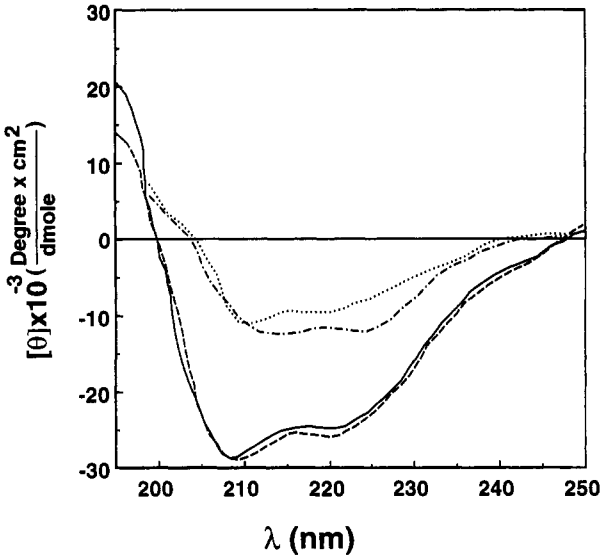

FIGURE 1: CD spectra of CecB and [3→35]CecB in methanol and in the presence of phospholipid vesicles. Spectra were taken as described in the Experimental Procedures section: —, CecB in methanol; – –, [3→35]CecB in methanol; – · –, CecB in the presence of PS/PC vesicles; ···, [3→35]CecB in the presence of PS/PC vesicles.

polypeptides, such as the bee venom melittin (Vogel, 1981), bombinin-like peptides (Gibson et al., 1986), pardaxin and its analogues (Shai et al., 1990, 1991), and the antimicrobial peptides alamethicin (Rizzo et al., 1987), magainin (Chen et al., 1988), and dermaseptin (Mor et al., 1991).

In the presence of acidic PS/PC vesicles (peptide/lipid molar ratio of 1:60), both CecB and [3→35]CecB exhibited typical double-minima spectra of α-helical peptides. However, low mean residual ellipticities $[\theta]_{222}$ of −11 900 and 8570 deg·cm²/dmol were calculated for CecB and [3→35]CecB, respectively, which correspond to fractional helicity values of 33% and 22%, respectively. These values are about 30–45% of the high fractional helicity in methanol (74%). It should be noted that the CD spectra of CecB and [3→35]CecB in the presence of vesicles were obtained at an optimal peptide/lipid molar ratio of 0.027 to avoid the interference of light scattering due to a high concentration of vesicles. Under these conditions, the amounts of peptides bound to vesicles as calculated from their binding isotherms (Figures 4 and 6) are 49% and 37% for CecB and [3→35]CecB, respectively. Therefore, the marked difference in their CD spectra, in the presence of vesicles, probably reflects the different levels of fractions bound.

Antibacterial Activity of CecB and Its Analogues. The antibacterial activities of CecB, [3→35]CecB, and their NBD and rhodamine derivatives were assessed utilizing inhibition zone assays, using both Gram-negative and Gram-positive bacteria. The results are summarized in Table 2. The data show that *B. mori* synthetic CecB and its fluorescent derivatives are highly active against *E. coli* and *B. megaterium*, but exhibit a lower or no effect on the growth of the other bacteria tested. The antibacterial activities of NBD- and rhodamine-labeled

Table 2: Lethal Concentrations (μM) of CecB and Its Analogues

bacterium	strain	CecB	NBD-CecB	Rho-CecB	[3→35]CecB	NBD-[3→35]CecB	Rho-[3→35]CecB
Bacillus megaterium	51.17	1.7	3.3	3.15	>207	>207	>207
Escherichia coli	MC 4100	0.35	3.30	3.15	25.9	34.5	154
Micrococcus luteus	53.45	>207	>207	>207	>207	>207	>207
Pseudomonas aeruginosa	A22	10	8.80	31.0	>207	>207	>207
Serratia marcescens	15.88	17.2	66	66	>207	>207	>207

CecB's were similar to those of CecB with respect to certain test bacteria and reduced for others (Table 2). For example, NBD-CecB retained 10–100% of its antibacterial activity with respect to the various test bacteria, while Rho-CecB varied from 10 to 50%. The labeled truncated derivatives, NBD-[3→35]CecB and Rho-[3→35]CecB, maintained 75% and 15%, respectively, of the activity of [3→35]CecB. Nevertheless, the relative specificity was conserved. The growth of *M. luteus* strain 53.45 was completely unaffected by CecB and its fluorescent analogues at concentrations up to 207 μM. Truncated [3→35]CecB and its rhodamine derivative exhibited reduced inhibitory activity against *E. coli* and did not affect the growth of the other four bacteria tested.

Binding to Bacteria and Erythrocytes. Rho-CecB and Rho-[3→35]CecB were used to elucidate whether intact and truncated CecB's can bind to bacteria and human erythrocytes. Figure 2 shows representative photomicrographs taken with an exposure time of 22 s. Since fluorescence intensity is highly dependent on appropriate focusing, the micrographs show only the intensively labeled population of bacteria. The data reveal that CecB bound *E. coli*, and to a lesser extent *S. marcescens*, but not human erythrocytes. While in the case of *E. coli* the labeling was homogeneous (by actual visualization this effect was more significant), it was not so for *S. marcescens*. In the latter case only some bacteria were intensively labeled, and others were labeled slightly or not at all. These results correlate with the higher potency of Rho-CecB to inhibit the growth of *E. coli* as compared to *S. marcescens* and with its inability to lyse human erythrocytes (Table 2). Furthermore, the reduced potency of Rho-[3→35]CecB to inhibit the growth of *E. coli* also correlates with the reduced intensity of the fluorescence of *E. coli* labeled with Rho-[3→35]CecB (Figure 2). Rho-ethanolamine (used as a control) did not bind to either bacteria or human erythrocytes. Whether the reduced ability of CecB to bind to *S. marcescens* was due to exogenous proteolytic digestion during the binding assay was determined by assessing the antimicrobial activity of CecB after its incubation with supernatant from *S. marcescens* culture, as described in the Experimental Procedures. CecB that was preincubated for up to 30 min with the supernatant was as active as the untreated peptide against *E. coli* (data not shown). Since the binding experiments entailed at most a 10 min exposure to culture supernatant, CecB was assumed to be intact and not degraded by proteinases, at least during the period of the binding experiments.

Localization of the Environment of the NBD Moiety. Since the fluorescence of NBD is very sensitive to its environment, it has been utilized previously for polarity and binding studies (Kenner & Aboderin, 1971; Frey & Tamm, 1990; Rapaport & Shai, 1991; Pouny & Shai, 1992). Herein, the fluorescence emission spectra of NBD-CecB, NBD-[3→35]CecB, and NBD–aminoethanol (a control) were monitored in aqueous solutions and in the presence of vesicles composed of either PC or PC/PS at pH 6.8. In these fluorometric studies, SUVs were used to minimize differential light-scattering effects (Mao & Wallace, 1984), and the lipid/peptide molar ratio was elevated (>3000:1) so that the spectral contributions of free peptide would be negligible. In buffer, NBD-CecB and NBD-[3→35]CecB exhibited a maximum of fluorescence emission at 545 ± 1 nm (Figure 3), which reflects a hydrophilic environment for the NBD moiety (Rajarathnam et al., 1989). However, when vesicles were added to the aqueous solutions containing NBD-CecB or NBD-[3→35]CecB, a blue shift in the emission maximum (toward 529 ± 1 nm) and an increase in the fluorescence intensity of the NBD group were observed for both peptides in the presence of PC/PS and for NBD-CecB only in the presence of PC vesicles. The change in the spectrum of the NBD group reflects its relocation to a more hydrophobic environment (Chattopadhyay & London, 1987). This blue shift suggests that penetration of the N-termini of the peptides was not as deep into the phospholipid environment as was observed for pore-forming polypeptides (emission maximum of 518–526 nm; Rapoport & Shai, 1992; Gazit & Shai, 1993b). It rather resembles that observed for an NBD group located at or near the surface of the membrane (emission maximum of 530–534 nm) (Chattopadhyay & London, 1987; Rajarathnam et al., 1989; Pouny et al., 1992). No shift was observed with the control, NBD–aminoethanol.

In order to investigate the influence of a transmembrane potential on the location of the NBD moiety, we performed the following experiment: PC or PC/PS SUVs, prepared in K^+ buffer, were added to 2 mL of K^+-free buffer (both defined in the Experimental Procedures section in the diffusion potential experiments). NBD-labeled cecropin (0.1 μM) was then added to the mixture, and the emission spectrum of the NBD group was recorded. The addition of a valinomycin solution (final concentration, 4 nM) created a negative diffusion potential inside the vesicles by a selective afflux of K^+ ions. Formation of a negative diffusion potential was confirmed by the quenching of the voltage sensitive dye, diS-C_2-5, under identical experimental conditions. The fluorescence emission spectrum, recorded as described above, was recorded again after 10 min of exposure to valinomycin. The establishment of a diffusion potential had no effect on the emission intensity or on the extent of the blue shift, demonstrating that the negative diffusion potential formed in the presence of valinomycin did not cause detectable changes in the probe's location. Note that, at the low peptide/lipid ratio used in this experiment, cecropin was unable to permeate the vesicles; thus it did not induce the dissipation of the diffusion potential existing within them.

Characterization of Binding Isotherms and Determination of Partition Coefficients. The fluorescent properties of the NBD moiety enabled the generation of binding isotherms for NBD-CecB and NBD-[3→35]CecB, from which partition coefficients could be calculated, as previously described (Rapaport & Shai, 1991). First, a fixed concentration (0.2 μM) of NBD-CecB and NBD-[3→35]CecB was titrated with the desired vesicles (e.g., PC or PS/PC for NBD-CecB and PS/PC for NBD-[3→35]CecB). Plots of the resulting increases in the fluorescence intensities of NBD-labeled peptides as a function of lipid/peptide molar ratios yielded conventional binding curves (Figure 4A for NBD-CecB with PC, Figure 5A for NBD-CecB with PS/PC, and Figure 6A

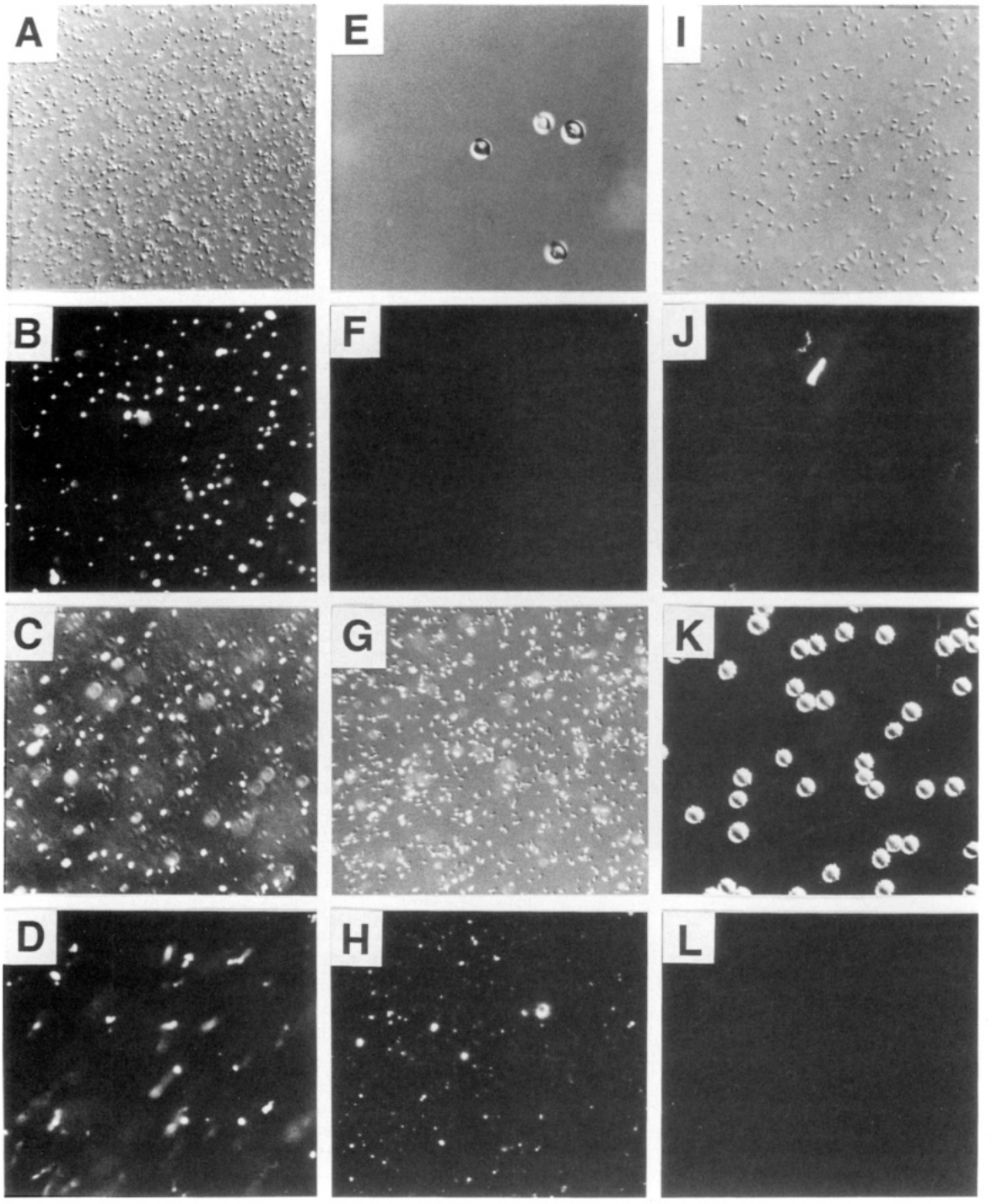

FIGURE 2: Binding of CecB and [3→35]CecB to bacteria and human erythrocytes. Early stationary phase bacteria and human erythrocytes were incubated with Rho-CecB (12.5 μM) or Rho-[3→35]CecB (12.5 μM) in 20 μL of PBS (pH 7.5) for 10 min and finally washed as described in the Experimental Procedures section. Plate designations: A, Rho-CecB with *E. coli* under regular light; B, Rho-CecB with *E. coli* under fluorescent irradiation; C, Rho-CecB with *S. marcescens* under regular light; D, Rho-CecB with *S. marcescens* under fluorescent irradiation; E, Rho-CecB with erythrocytes under regular light; F, Rho-CecB with erythrocytes under fluorescent irradiation; G, Rho-[3→35]CecB with *E. coli* under regular light; H, Rho-[3→35]CecB with *E. coli* under fluorescent irradiation; I, Rho-[3→35]CecB with *S. marcescens* under regular light; J, Rho-[3→35]CecB with *S. marcescens* under fluorescent irradiation; K, Rho-[3→35]CecB with erythrocytes under regular light; L, Rho-[3→35]CecB with erythrocytes under fluorescent irradiation.

for NBD-[3→35]CecB with PC/PS). Since the concentrations of the NBD-labeled peptides in the mixtures were low, the peptides were assumed not to disrupt the bilayer structure. When unlabeled CecB or [3→35]CecB was titrated with lipids, up to the maximal concentration used with NBD-labeled peptides, the fluorescence intensities of the solutions, after subtraction of the contribution of the vesicles, remained unchanged.

The curves obtained by plotting X_b* (the molar ratio of bound peptide per 60% of the total lipid) vs C_f (the equilibrium concentration of free peptide in the solution) are referred to as the conventional binding isotherms. The experimental binding isotherms of the interaction of NBD-CecB with PC (Figure 4B) and of NBD-CecB and NBD-[3→35]CecB with PC/PS (Figures 5B and 6B, respectively) SUVs were determined. The surface partition coefficients were estimated

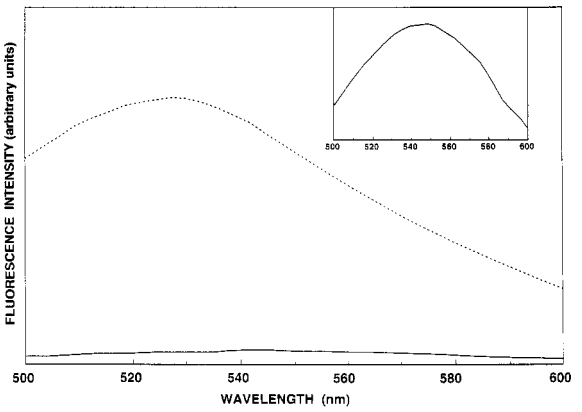

FIGURE 3: Fluorescence emission spectra of NBD-CecB. Spectra of 0.1 μM NBD-CecB in buffer (50 mM Na_2SO_4/25 mM HEPES–sulfate, pH 6.8) (—) or in the presence of 350 μM PC/PS SUVs (- - -). The excitation wavelength was 470 nm, and emission was scanned from 500 to 600 nm. Inset: Magnification of the signal obtained with NBD-CecB in buffer.

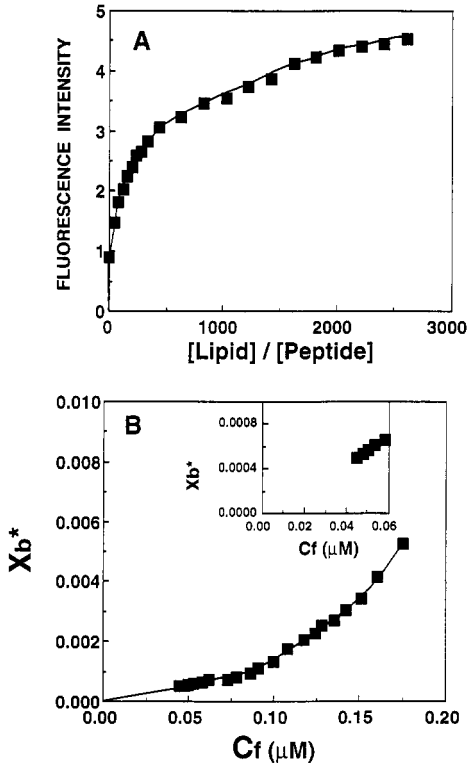

FIGURE 4: Increase in the fluorescence of NBD-CecB upon titration with PC vesicles (A) and the resulting binding isotherm (B). (A) NBD-CecB (0.2 μM) in 50 mM Na_2SO_4/25 mM HEPES–sulfate was titrated with PC vesicles at 24 °C; the excitation wavelength was 470 nm and emission was monitored at 530 nm. (B) Binding isotherm derived from Figure 4A by plotting X_b* (molar ratio of bound peptide per 60% of lipid) vs C_f (equilibrium concentration of free peptide in the solution). Inset: Values at low C_f concentrations.

by extrapolating the initial slopes of the curves to C_f values of zero. The estimated surface partition coefficients, K_p*, of NBD-CecB were $(1.1 \pm 0.2) \times 10^4$ and $(1.2 \pm 0.3) \times 10^5$ M^{-1} with PC and PC/PS vesicles, respectively, and that of NBD-[3→35]CecB was $(1.2 \pm 0.2) \times 10^5$ M^{-1} with PC/PS vesicles (four measurements each). The 10-fold increase in K_p* with PS/PC as compared to PC vesicles may result from electrostatic interactions between the acidic head group of PS and the positive charges of CecB. These K_p* values are within the range of those obtained for other membrane-permeating bioactive peptides, such as melittin and its derivatives

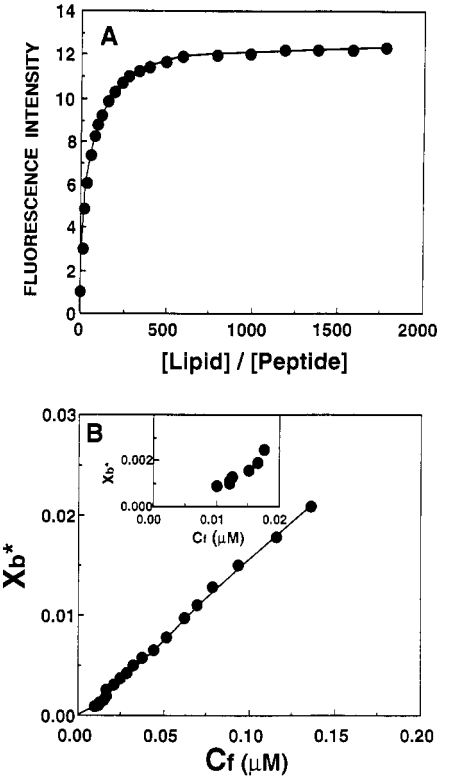

FIGURE 5: Increase in the fluorescence of NBD-CecB upon titration with PS/PC vesicles (A) and the resulting binding isotherm (B). (A) NBD-CecB (0.2 μM) in 50 mM Na_2SO_4/25 mM HEPES–sulfate was titrated with PS/PC at 24 °C; the excitation wavelength was 470 nm and emission was monitored at 530 nm. (B) Binding isotherm derived from Figure 5A (see legend of Figure 4).

(Stankowski & Schwarz, 1990), the *Staphylococcus* δ-toxin (Thiaudière et al., 1991), the antibiotic dermaseptin (Pouny et al., 1992), and pardaxin and its analogues (Rapaport & Shai, 1991).

The shape of a binding isotherm of a peptide can provide information on the organization of the peptide within the membrane (Schwarz et al., 1986, 1987). The binding isotherms of NBD-CecB and NBD-[3→35]CecB in PC/PS vesicles are almost straight lines, which indicates a simple adhesion process, while those of NBD-CecB in PC vesicles bend slightly upward. This upward curvature suggests a slight self-association of peptide monomers. The binding isotherms of NBD-CecB and NBD-[3→35]CecB are similar to those obtained with the antimicrobial dermaseptin peptide (Pouny et al., 1992), but very different from those obtained with pore-forming polypeptides such as the antimicrobial peptide alamethicin (Rizzo et al., 1987), the neurotoxin pardaxin and its analogues (Rapaport & Shai, 1991), the α-5 segment of *B. thuringiensis* CryIIIA δ-endotoxin (Gazit & Shai, 1993a), and helix 2 of *B. thuringiensis* var. *israelensis* cytolytic toxin (Gazit & Shai, 1993b). The isotherms of the latter pore-forming peptides display an initial lag, i.e., initially the curves are flat, but they rise sharply once a threshold concentration is achieved. This is consistent with a process whereby peptides first incorporate into the membrane, and once inside the membrane they aggregate to form a pore (Schwarz et al., 1986, 1987).

Resonance Energy Transfer (RET) Experiments. To evaluate whether CecB can self-associate within membranes, RET measurements were performed with NBD-labeled (energy donors) and Rho-labeled peptides (energy acceptors), as described previously (Rapaport & Shai, 1992). Addition

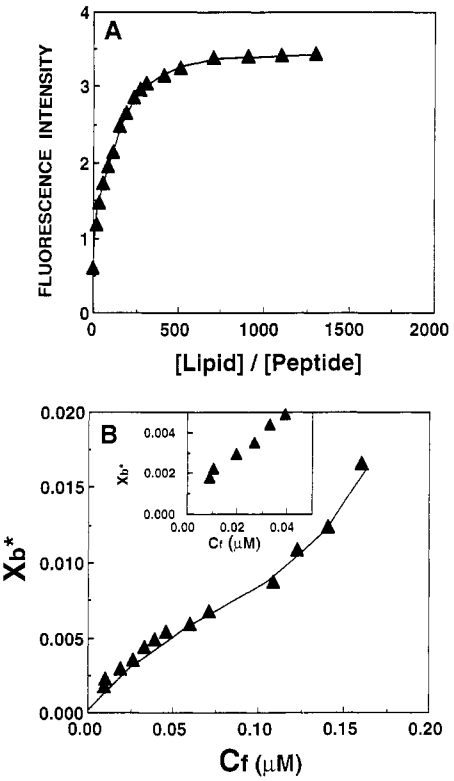

FIGURE 6: Increase in the fluorescence of NBD-[3→35]CecB upon titration with PS/PC vesicles (A) and the resulting binding isotherm (B). (A) NBD-[3→35]CecB (0.2 μM) in 50 mM Na_2SO_4/25 mM HEPES–sulfate was titrated with PS/PC at 24 °C; the excitation wavelength was 470 nm and emission was monitored at 530 nm. (B) Binding isotherm derived from Figure 6A (see legend for Figure 4).

of Rho-labeled CecB or [3→35]CecB (final concentrations of 0.02–0.5 μM) to NBD-labeled peptides (0.05 μM) in the presence of PC or PS/PC phospholipid vesicles (100 μM) quenched the donor's emission and increased the acceptor's emission, which is consistent with energy transfer. In control experiments, no change in the emission spectrum of NBD was observed when equal amounts of unlabeled peptides rather than Rho-labeled peptides were added (data not shown). Similar experiments were performed with mixtures containing NBD-CecB as a donor and Rho-pardaxin as an acceptor. The resulting curves of the experimentally derived percentage of energy transfer vs the various molar ratios of bound acceptor (C_b)/lipid are depicted in Figures 7 and 8 for PC and PS/PC vesicles, respectively. Figure 7 depicts the percentage of energy transfer between donor-/acceptor-labeled pardaxins for comparison. A curve corresponding to a random distribution of monomers that assumes a surface density of donor (donor/lipid) to be 0.01, as calculated for the NBD/Rho (donor/acceptor) pair (Fung & Stryer, 1978), and an R_0 of 51.1 Å, as calculated for the NBD/Rho pair (Gazit & Shai, 1993b), is inserted. The amounts of lipid-bound acceptors (Rho-peptides), C_b, at the various Rho-peptide concentrations were calculated from the binding isotherms of the corresponding NBD-labeled peptides, as previously described (Pouny et al., 1992). First, the fractions of bound acceptor, f_b, were calculated for the various acceptor/lipid molar ratios tested. Next, it was possible to calculate the fraction bound, C_b (C_b = [μM acceptor]f_b).

The results obtained in the RET experiments are similar to those obtained with the antimicrobial peptide dermaseptin (Pouny et al., 1992), rather than to those obtained with the pore-forming polypeptides the neurotoxin pardaxin (Figure 7; Rapaport & Shai, 1992) or helix 2 of Bti toxin (Gazit &

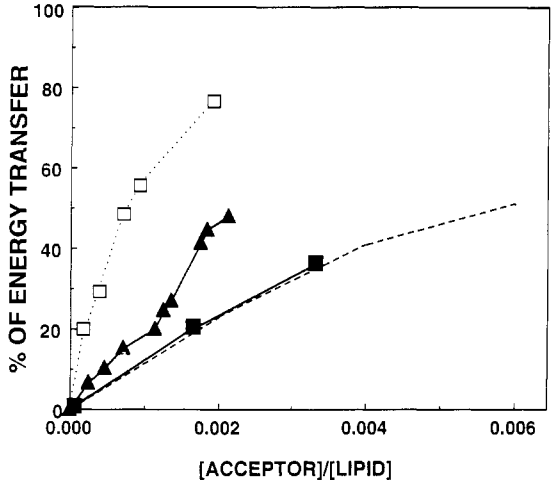

FIGURE 7: Theoretically and experimentally derived percentage of energy transfer vs bound acceptor/lipid molar ratio, using PC vesicles. The spectra of NBD-CecB (0.1 μM), the donor peptide, was determined in the presence or absence of various concentrations of the acceptor peptide, Rho-CecB. Each spectrum was recorded in the presence of PC vesicles (100 μM) in 50 mM Na_2SO_4/25 mM HEPES–sulfate at pH 6.8. The excitation wavelength was set at 470 nm; emission was scanned from 500 to 600 nm. The amount of lipid-bound acceptor (Rho-peptides), C_b, at various acceptor concentrations was calculated from the binding isotherms as described in the Experimental Procedures section. Designations are as follows: ▲, NBD-CecB/Rho-CecB; ■, NBD-CecB/Rho-pardaxin; □, fluorescein-pardaxin/Rho-pardaxin; - - -, random distribution of the monomers (Fung & Stryer, 1978), assuming an R_0 of 51.1 Å (Gazit & Shai, 1993b).

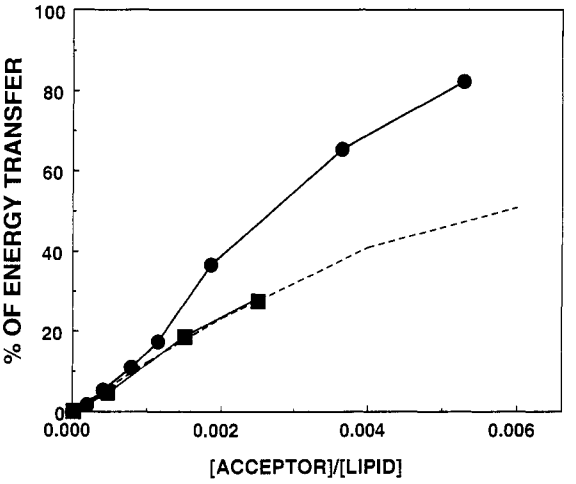

FIGURE 8: Theoretically and experimentally derived percentage of energy transfer vs bound acceptor/lipid molar ratio using PC/PS vesicles. See the legend for Figure 7, except that PC/PS vesicles replaced PC vesicles. Designations are as follows: ●, NBD-CecB/Rho-CecB; ■, NBD-CecB/Rho-pardaxin; - - -, random distribution of the monomers (Fung & Stryer, 1978).

Shai, 1993b). In order to investigate the influence of transmembrane potential on the self-aggregation process, we performed the following experiment: PC/PS SUVs, prepared in K^+ buffer, were added to 2 mL of K^+-free buffer (both defined in the Experimental Procedures section in the diffusion potential experiments). NBD-labeled cecropin (0.1 μM) was then added to the mixture followed by the addition of acceptor, Rho-cecropin, which caused quenching of the NBD fluorescence. The addition of a valinomycin solution (final concentration, 4 nM) created a negative diffusion potential inside the vesicles by a selective afflux of K^+ ions. Formation of a negative diffusion potential was confirmed by the quenching of the voltage sensitive dye, diS-C_2-5, under identical

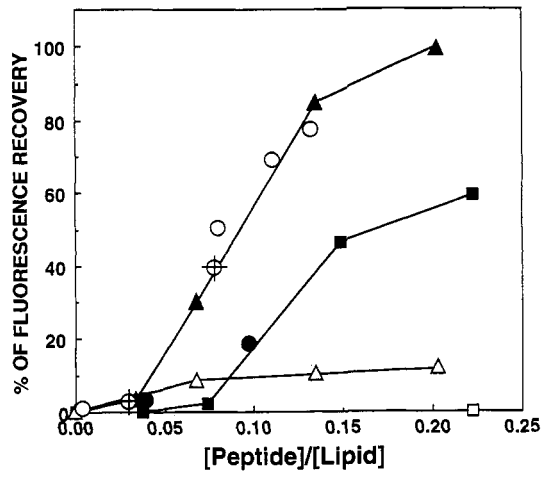

FIGURE 9: Maximal dissipation of the diffusion potential in vesicles induced by the peptides. The peptides were added to isotonic K^+-free buffer containing SUVs preequilibrated with the fluorescent dye diS-C_2-5 and valinomycin. Fluorescence recovery, measured 10–20 min after mixing the peptides with the vesicles, is depicted. Designations are as follows: ▲, CecB with PC/PS SUV; ■, [3→35]CecB with PC/PS SUV; △, CecB with PC SUV; □, [3→35]CecB with PC SUV; ○, NBD-CecB with PC/PS; ⊗, Rho-CecB with PC/PS; ●, NBD-[3→35]CecB with PC/PS.

experimental conditions. Fluorescence emission spectra, recorded as described above, were recorded at time 0 and again after 10 min of exposure to valinomycin. The establishment of a diffusion potential had no effect on the degree of quenching, demonstrating that the negative diffusion potential formed in the presence of valinomycin did not cause detectable changes in the probes' intermolecular distances. Note that, at the low peptide/lipid ratio used in this experiment, cecropin was unable to permeate the vesicles; thus it did not induce the dissipation of the diffusion potential existing within them.

Membrane Permeability Induced by the Peptides. CecB, [3→35]CecB, and their fluorescent derivatives were examined for their efficacy in perturbing lipid packing and causing the leakage of vesicular contents, by utilizing the dissipation of diffusion potential assay. Increasing concentrations of CecB or its analogues were mixed either with PC or with PS/PC SUVs that had been pretreated with the fluorescent, potential sensitive dye diS-C_2-5 and valinomycin. Recovery of fluorescence was monitored as a function of time and usually occurred within 10–25 min. Maximal activity of CecB and its analogues was plotted vs peptide/lipid molar ratios (Figure 9). Each point represents the mean of three separate experiments, with a standard deviation of ~5%. High perturbing activity of CecB was revealed with PS/PC, in contrast to the low level observed with PC vesicles (Figure 9). For example, at the lipid/CecB molar ratio of 0.14, ~90% and 10% of permeating activity are observed for PS/PC and PC vesicles, respectively. The truncated [3→35]CecB and its fluorescent analogues permeate acidic PC/PS vesicles, but not zwitterionic ones, which correlates with their inability to bind PC vesicles. However, although [3→35]CecB and CecB bind PS/PC equally, the truncated [3→35]CecB has a reduced permeating activity. All of the fluorescently labeled analogues exhibited the same activity as their parent molecules (Figure 9). The minimal activity of CecB was observed with PS/PC vesicles using peptide/lipid molar ratios of ~0.03:1, corresponding to a 33:1 lipid/peptide molar ratio. If we assume a vesicle size of 20–50 nm (as measured by utilizing an electron microscope), and a random distribution of peptide monomers between vesicles, then >110 peptide molecules are bound to one vesicle. This number is higher than that estimated for the pore-forming polypeptides, the neurotoxin pardaxin (Rapaport & Shai, 1992), and helix 2 of Bti toxin (Gazit & Shai, 1993b), in which a mean of as low as 2–4 molecules can induce a dissipation of diffusion potential from vesicles.

DISCUSSION

Although the precise mechanism of the antibacterial activity of polycationic amphipathic α-helical peptides is not yet known, accumulating data suggest that peptide–lipid interactions appear to be an essential step for their activity. Such interactions have been proposed to destroy the energy metabolism of the target organism by increasing the permeability of energy-transducing membranes (Okada & Natori, 1985; Zasloff, 1987; Westerhoff et al., 1989). Thus, the mechanisms by which various antibacterial peptides permeate model phospholipid membranes were investigated.

Herein, a fluorometric approach was utilized to investigate the interaction of CecB, present in the silkworm *B. mori*, with model phospholipid membranes (at lipid/peptide molar ratios up to ~3000:1), bacteria, and human erythrocytes. CecB and its [3→35]CecB analogue were synthesized and selectively labeled at their N-terminal amino acids with either NBD or Rho. By utilizing model phospholipid membranes, the following characteristics of CecB were determined: (i) the partition coefficients of NBD-labeled cecropins with vesicles composed of zwitterionic PC or acidic PS/PC phospholipids; (ii) the organization state of CecB when bound to PC or PS/PC vesicles, in the presence or absence of membrane potential; and (iii) the ability of the peptides to permeate phospholipid vesicles composed of PC or PS/PC. The secondary structure of the peptides in an aprotic solvent was also determined. To visualize binding of the peptides to bacteria and human erythrocytes, fluorescently labeled analogues were used. The mode of action of CecB on model membranes is discussed with regard to the proposed antibacterial mechanisms of other antibacterial peptides.

The data presented herein suggest that a membrane disintegration, rather than a channel- or a pore-forming mechanism, is the initial predominant event leading to membrane permeation. This suggestion is based on the following observations: (i) The binding isotherm of NBD-CecB obtained with the susceptible acidic phospholipid (PS/PC) vesicles is almost a straight line, which indicates a simple adhesion process, whereas in zwitterionic (PC) vesicles, which are less susceptible, the shape bends slightly upward, which indicates a slight self-association of peptide monomers (Figures 4B and 5B). However, the increase in the slope of the binding isotherm of CecB in PC vesicles is much lower than that observed for channel-forming peptides, such as alamethicin (Rizzo et al., 1987), pardaxin (Rapaport & Shai, 1991), and helix 2 of Bti δ-endotoxin (Gazit & Shai, 1993b). With these channel-forming peptides, their binding slopes increased >100-fold, which reflects a cooperative binding at low peptide/lipid molar ratios, hence suggesting a barrel stave mechanism (Ehrenstein & Lecar, 1977) for their channel-forming properties. The barrel stave model involves three steps. In the first step, monomers dissolved in solution bind to the membrane. Next, these monomers insert into the lipid bilayer. Finally, the monomers aggregate into a barrel-like structure in which a central aqueous pore surrounded by protein is formed. This pore increases in diameter through the progressive recruitment of additional monomers. (ii) The membrane-permeating activity of CecB on PC vesicles was lower than

on PS/PC ones, even at a high peptide/lipid molar ratio, which corresponded to >200 peptide monomers per vesicle when a random distribution of peptide monomers was assumed within the vesicles (Figure 9). Furthermore, even with PS/PC vesicles, initial permeating activity with CecB was observed when a mean of >100 peptide monomers bound to a vesicle (calculated assuming a vesicle size of 20–50 nm, as observed utilizing electron microscopy). These numbers are significantly higher than those estimated (4–10 peptide monomers per vesicle) for the pore-forming peptides, pardaxin (Shai et al., 1990, 1991), and helix 2 of Bti δ-endotoxin (Gazit & Shai, 1993b). (iii) In RET experiments, at low CecB/lipid molar ratios, a slight energy transfer occurred between donor/acceptor CecB with zwitterionic PC vesicles, but not with the more susceptible acidic PS/PC vesicles (Figure 7). Furthermore, the RET values were lower than those observed for pardaxin (Figure 7) or helix 2 of Bti toxin (Gazit & Shai, 1993b). With both PC and PC/PS vesicles, significant energy transfer between donor/acceptor CecB monomers occurred only after a threshold peptide/lipid molar ratio was achieved. However, when utilizing NBD-CecB as a donor, energy transfer was not observed when the acceptor molecule, Rho, was attached to pardaxin. (iv) Observations i and iii were not affected by membrane polarization caused by the presence of a diffusion potential. (v) CecB is a highly charged molecule (nine positively charged and three negatively charged amino acids), and it forms an amphipathic α-helix. Therefore, it is energetically unlikely that such charged molecules will stay as monomers within the highly hydrophobic core of the lipid membrane. A more likely situation is one in which the monomers lie on the surface of the membrane, where hydrophobic residues are oriented toward the hydrocarbon chains of the phospholipids and the hydrophilic residues interact with the water molecules or the charged head groups of the phospholipids.

The self-association property of CecB at high peptide/lipid molar ratios may explain why, at relatively high concentrations, other cecropin homologues form single channels in planar lipid membranes (Christensen et al., 1988). The formation of such channels could occur if some of the monomers transverse the membrane and form a bundle, such that their outwardly directed, hydrophobic surfaces interact with the lipid core of the membrane, while their inwardly facing, hydrophilic surfaces produce a conducting pore (Inouye, 1974; Guy & Seetharamulu, 1986; Greenblatt et al., 1985). Such a model was recently constructed for *H. cecropia* cecropin A (Durell et al., 1992).

The non-ion channel formation mechanism proposed to be the major mode of interaction of cecropin with phospholipid membranes appears to be a common destructive mechanism for other amphipathic, α-helical antibacterial peptides, such as magainin (Matsuzaki et al., 1991; Bechinger et al., 1991, 1992), cecropin A (Steiner et al., 1988), and dermaseptin (Pouny et al., 1992). That magainin lies on the surface of phospholipid layers rather than forming transmembrane bundles, as revealed by solid state NMR (Bechinger et al., 1991, 1992), and that dermaseptin randomly distributes rather than self-aggregates in its membrane-bound state (Pouny et al., 1992) can be explained by the following proposed mechanism of antibacterial activities of peptides: The site most likely to be the target of membrane-permeating antibacterial peptides is the inner membrane of bacteria, which typically contains the electron transport chain and the enzymatic apparatus necessary for oxidative phosphorylation (Westerhoff et al., 1989). To reach this membrane, the peptides have to traverse the bacterial wall, the outer surface of which contains, in the case of Gram-negative bacteria, lipopolysaccharides (LPS) and, in the case of Gram-positive bacteria, acidic polysaccharides (teichoic acids), giving the surfaces of both Gram-positive and Gram-negative bacteria a negative charge (Brock, 1974). Therefore, the net positive charge of the antibacterial peptides should facilitate their binding to bacteria. If high cooperativity in binding then occurs, the majority of the peptides should remain in the outer surface and form large aggregates. Such aggregates would impede the diffusion of monomers into the inner membrane. Alternatively, the presence of monomeric forms of the peptides on the outer surface of bacteria, which is characteristic of simple adhesion, should allow the monomers to readily diffuse into the inner membrane and to permeate it. This suggestion may explain why the shark repellent pardaxin, which is a highly potent membrane-permeating polypeptide with a tendency to cooperatively bind to membranes and to lyse cells and erythrocytes (Lazarovici et al., 1986; Rapaport & Shai, 1992), cannot inhibit the growth of bacteria.

The proposed mechanism is in agreement with those proposed previously for the interaction of the following: (i) polycations, such as polymyxins and macrophage cationic proteins (MCPs), with the outer membrane of *P. aeruginosa* (Sawyer et al., 1988), which is highly susceptible to CecB; (ii) defensins with *E. coli* (Lehrer et al., 1989); and (iii) magainin with *S. typhimurium* (Rana et al., 1991). According to the previously proposed mechanisms, the polycations displace divalent cations that cross-bridge adjacent LPS molecules. The displacement caused by the large polycations disrupts the outer membrane of the bacterium and, consequently, increases the permeability of the bacterial wall toward the inner membrane. That the N-terminal fluorescently labeled CecB analogues preserved their membrane-permeating activity (Figure 9), but had reduced antibacterial activity in most cases (Table 2), may suggest that the neutralization of the free N-terminal amino group of CecB affects its binding to bacteria, rather than its ability to permeate the inner phospholipid membrane. That binding of large amounts of CecB to bacteria or human erythrocytes is required to induce lytic effects was revealed by the direct correlation between the antibacterial activity of CecB or its truncated analogues and the ability of their Rho-labeled analogues to interact with bacteria and human red blood cells. Rho-CecB bound strongly to the CecB sensitive *E. coli*, but exhibited a lesser extent of binding to the more resistant insect pathogen *S. marcescens* (Figure 2). Interestingly, while Rho-CecB bound *E. coli* homogeneously, its binding to *S. marcescens* was heterogeneous. It bound strongly to some, while the other members of the same population were essentially unlabeled. By actual visualization this effect was even more significant, since fluorescence intensity is highly dependent on appropriate focusing.

The heterogeneity of Rho-CecB binding may be due to different stages of development or surface properties of the target bacteria. Furthermore, only traces of Rho-[3→35]-CecB bound to *S. marcescens*, for which it has no detectable activity. Rho-CecB does not bind to or exhibit hemolytic activity against human erythrocytes (Figure 2). The outer leaflet of human erythrocytes is composed of zwitterionic (PC) and sphingomyelin phospholipids (Verkleij et al., 1973). Thus, the inability CecB to bind to human erythrocytes may be explained by the finding that the peptide has a low affinity for zwitterionic PC phospholipid vesicles compared to acidic PC/PS vesicles (Figures 4 and 5). However, we cannot rule

out the possibility that the amount of bound cecropin is very low and cannot be detected under our experimental conditions. Although radioactively labeled cecropin A has been shown not to bind to erythrocytes, it binds to both the cecropin A sensitive bacterium *E. coli* and the cecropin A resistant *B. thuringiensis* (Steiner et al., 1988). However, binding techniques utilizing radiolabeled probes, unlike those utilizing fluorescently labeled ones, do not allow the detection of heterogeneous vs homogeneous binding. The differences in the binding of CecB to different bacteria may be due in part to differences in the composition of the bacterial wall. As an example, within Gram-negative bacteria, the structure of LPS is highly variable from one species to another, especially in the core oligosaccharide structure and in the O-antigenic polysaccharide (Sleytr et al., 1988). The LPS structure was shown to have an important role in the interaction between magainin, an antibacterial peptide, and the Gram-negative bacteria *S. typhimurium* (Rana et al., 1991).

It should be noted that while Rho-[3→35]CecB binds *E.coli* significantly (Figure 2), its antibacterial activity is markedly reduced (Table 2). This may be explained by the finding that NBD-CecB and NBD-[3→35]CecB have identical partition coefficients with acidically charged phospholipids (1.2×10^5 M^{-1}, Figures 5 and 6). Therefore, they both have the capacity to bind the acidically charged outer surface of the bacteria and to diffuse to the inner target membrane. However, since [3→35]CecB has significantly reduced membrane-permeating activity (Figure 9), this should affect its ability to permeate the inner membrane of the bacteria.

It should be noted that, contrary to the previous findings of others (Morishima et al., 1990), *M. luteus* was completely resistant to *B. mori* CecB (Table 2) and its derivatives, a difference that may be partially strain related.

In summary, the non-cooperativity in the binding of CecB to phospholipid membranes and its inability to associate on the surface of acidically charged membranes independent of membrane polarization suggest that CecB binds phospholipid membranes preferentially as monomers lying on the surface, rather than as bundles of monomers that form a transmembrane pore. A similar mechanism appears to be used by other amphipathic α-helical antibacterial peptides, but not by membrane-permeating amphipathic α-helical peptides that do not manifest antibacterial activity. We speculate that this non-cooperative binding of the peptides to the surface of outer bacterial membranes (i.e., no aggregation of CecB monomers) may assist them in efficiently diffusing into the inner target membranes.

REFERENCES

Andreu, D., Merrifield, R. B., Steiner, H., & Boman, H. G. (1985) *Biochemistry 24*, 1683–1688.

Bartlett, G. R. (1959) *J. Biol. Chem. 234*, 466–468.

Bechinger, B., Kim, Y., Chirlian, L. E., Gesell, J., Neumann, J. M., Montal, M., Tomich, J., Zasloff, M., & Opella, S. J. (1991) *J. Biomol. NMR 1*, 167–173.

Bechinger, B., Zasloff, M., & Opella, S. J. (1992) *Biophys. J. 62*, 12–14.

Beschiaschvili, G., & Seelig, J. (1990) *Biochemistry 29*, 52–58.

Bessalle, R., Kapitovsky, A., Gorea, A., Shalit,I., & Fridkin, M. (1990) *FEBS Lett. 274*, 151–155.

Boman, H. G. (1991) *Cell 65*, 205–207.

Boman, H. G., & Hultmark, D. (1987) *Annu. Rev. Microbiol. 41*, 103–126.

Brey, P. T., Lee, W.-J., Yamakawa, M., Koizumi, Y., Perrot, S., François, M., & Ashida, M. (1993) *Proc. Natl. Acad. Sci. U.S.A. 90*, 6275–6279.

Brock, T. D. (1974) *Biology of Microorganisms*, 2nd ed., Prentice-Hall Inc., Englewood Cliffs, NJ.

Chattopadhyay, A., & London, E. (1987) *Biochemistry 26*, 39–45.

Chen, Y. H., Yang, J. T., & Chau, K. H. (1974) *Biochemistry 13*, 3350–3359.

Chen, H. C., Brown, J. H., Morell, J. L., & Huang, C. M. (1988) *FEBS Lett. 236*, 461–466.

Christensen, B., Fink, J., Merrifield, R. B., & Mauzerall, D. (1988) *Proc. Natl. Acad. Sci. U.S.A. 85*, 5072–5076.

Durell, S. R., Raghunathan, G., & Guy, H. R. (1992) *Biophys. J. 63*, 1623–1631.

Ehrenstein, G., & Lecar, H. (1977) *Q. Rev. Biophys. 10*, 1–34.

Frey, S., & Tamm, L. K. (1990) *Biochem. J. 272*, 713–719.

Fung, B. K.-K., & Stryer, L. (1978) *Biochemistry 17*, 5241–5248.

Gazit, E., & Shai, Y. (1993a) *Biochemistry 32*, 3429–3436.

Gazit, E., & Shai, Y. (1993b) *Biochemistry 32*, 12363–12371.

Gibson, B. W., Poulter, L., Williams, D. H., & Maggio, J. E. (1986) *J. Biol. Chem. 261*, 5341–5349.

Greenblatt, R. A., Blatt, Y., & Montal, M. (1985) *FEBS Lett. 193*, 125–134.

Greenfield, N., & Fasman, G. D. (1969) *Biochemistry 8*, 4108–4116.

Guy, H. R., & Seetharamulu, P. (1986) *Proc. Natl. Acad. Sci. U.S.A. 83*, 508–512.

Holak, T. A., Engström, A., Kraulis, P. J., Lindeberg, G., Bennich, H., Jones, T. A., Gronenborn, A. M., & Clore, G. M. (1988) *Biochemistry 27*, 7620–7629.

Hultmark, D. (1993) *Trends Genet. 9*, 178–183.

Hultmark, D., Steiner, H., Rasmuson, T., & Boman, H. G. (1980) *Eur. J. Biochem. 106*, 7–16.

Hultmark, D., Engström, A., Bennich, H., Kapur, R., & Boman, H. G. (1982) *Eur. J. Biochem. 127*, 207–217.

Inouye, M. (1974) *Proc. Natl. Acad. Sci. U.S.A., 71*, 2396–2400.

Kenner, R., & Aboderin, A. (1971) *Biochemistry 10*, 4433–4440.

Lazarovici, P., Primor, N., & Loew L. M. (1986) *J. Biol. Chem. 261*, 8243–8248.

Lee, W.-J., & Brey, P. T. (1994) *Anal. Biochem. 217*, 231–235.

Lee, J.-Y., Boman, A., Chauanxin, S., Andersson, M., Jörnvall, H., Mutt, V., & Boman, H. G. (1989) *Proc. Natl. Acad. Sci. U.S.A. 86*, 9159–9162.

Lehrer, R. I., Barton, A., Daher, K. A., Harwig, S. S., Ganz, T., & Selsted, M. E. (1989) *J. Clin. Invest. 84*, 553–561.

Loew, L. M., Rosenberg, I., Bridge, M., & Gitler, C. (1983) *Biochemistry 22*, 837–844.

Mao, D., & Wallace, B. A. (1984) *Biochemistry 23*, 2667–2673.

Matsuzaki, K., Harada, M., Funakoshi, S., Fujii, N., & Miyajima, K. (1991) *Biochim. Biophys. Acta 1063*, 162–170.

Merrifield, R. B., Vizioli, L. D., & Boman, H. G. (1982) *Biochemistry 21*, 5020–5031.

Mor, A., Nguyen, V. H., Delfour, A., Migliore-Samour, D., & Nicolas, P. (1991) *Biochemistry 30*, 8824–8830.

Morishima, I., Suginaka, S., Ueno, T., & Hirano, H. (1990) *Comp. Biochem. Physiol. 95A*, 551–554.

Okada, M., & Natori, S. (1985) *Biochem. J. 229*, 453–458.

Papahadjopoulos, D., & Miller, N. (1967) *Biochim. Biophys. Acta 135*, 624–638.

Pouny, Y., & Shai, Y. (1992) *Biochemistry 31*, 9482–9490.

Pouny, Y., Rapaport, D., Mor, A., Nicolas, P., & Shai, Y. (1992) *Biochemistry 31*, 12416–12423.

Rajarathnam, K., Hochman, J., Schindler, M., & Ferguson-Miller, S. (1989) *Biochemistry 28*, 3168–3176.

Rana, F. R., Macias, E. A., Sultany, C. M., Modzrakowski, M. C., & Blazyk, J. (1991) *Biochemistry 30*, 5858–5866.

Rapaport, D., & Shai Y. (1991) *J. Biol.Chem. 266*, 23769–23775.

Rapaport, D., & Shai, Y. (1992) *J. Biol. Chem. 267*, 6502–6509.

Rizzo, V., Stankowski, S., & Schwarz, G. (1987) *Biochemistry 26*, 2751–2759.
Schwarz, G., Stankowsky, S., & Rizzo, V. (1986) *Biochim. Biophys. Acta 861*, 141–151.
Schwarz, G., Gerke, H., Rizzo, V., & Stankowski, S. (1987) *Biophys. J. 52*, 685–692.
Shai, Y., Bach, D., & Yanovsky, A. (1990) *J. Biol. Chem. 265*, 20202–20209.
Shai, Y., Hadari, Y. R., & Finkels, A. (1991) *J. Biol. Chem. 266*, 22346–22354.
Sims, P. J., Waggoner, A. S., Wang, C. H., & Hoffmann, J. R. (1974) *Biochemistry 13*, 3315–3330.
Sleytr, U. B., Messner, P., Minnikin, D. E., Heckels, J. E., Virji, M., & Russell, R. B. B. (1988) in *Bacterial Cell Surface Techniques* (Handcock, I., & Poxton, I., Eds.) John Wiley & Sons Ltd., London.
Stankowsky, S., & Schwarz, G. (1990) *Biochim. Biophys. Acta 1025*, 164–172.
Steiner, H., Hultmark, D., Engström, A., Bennich, H., & Boman, H. G. (1981) *Nature 292*, 246–248.
Steiner, H., Andreu, D., & Merrifield, R. B. (1988) *Biochim. Biophys. Acta 939*, 260–266.
Thiaudière, E., Siffert, O., Talbot, J. C., Bolard, J., Alouf, J. E., & Dufourcq, J. (1991) *Eur. J. Biochem. 195*, 203–213.
Verkleij, A. J., Zwaal, R. F. A., Roelofsen, B., Comfurius, P., Kastelijn, D., & Van Deenen, L. L. M. (1973) *Biochim. Biophys. Acta 323*, 178–193.
Vogel, H. (1981) *FEBS Lett. 134*, 37–42.
Wade, D., Boman, A., Wåhlin, C. M., Drain, D., Andreu, D., Boman, H. G., & Merrifield, R. B. (1990) *Proc. Natl. Acad. Sci. U.S.A. 87*, 4761–4765.
Westerhoff, H. V., Juretic, D., Hendler, R. W., & Zasloff, M. (1989) *Proc. Natl. Acad. Sci. U.S.A. 86*, 6597–6601.
Wu, C. S. C., Ikeda, K., & Yang, J. T. (1981) *Biochemistry 20*, 566–570.
Zasloff, M. (1987) *Proc. Natl. Acad. Sci. U.S.A. 84*, 5449–5453.